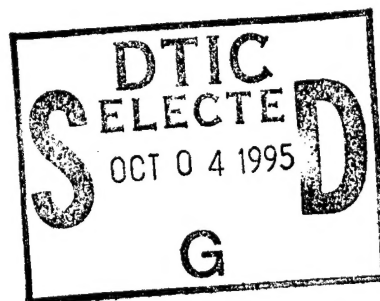PL-TR-95-2112

DMSP Sensor Fusion Auroral E-layer Algorithm: Functional Description

Robert E. Daniell, Jr.

Computational Physics, Inc.
240 Bear Hill Road, Suite 202A
Waltham, MA   02154

DTIC
SELECTED
OCT 0 4 1995
G
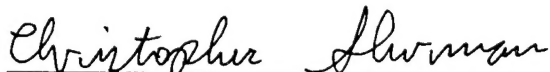
18 August 1995

Final Report
19 July 1991 – 19 July 1995

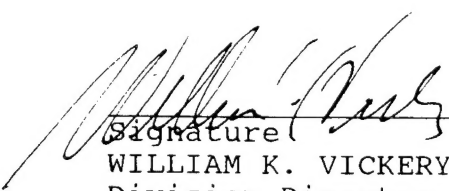Approved for public release; distribution unlimited

19951002 045

PHILLIPS LABORATORY
Directorate of Geophysics
AIR FORCE MATERIEL COMMAND
HANSCOM AFB, MA 01731-3010

"This technical report has been reviewed and is approved for publication"

Christopher Sherman
Signature
CHRISTOPHER SHERMAN
Contract Manager

James C. Bates (FOR)
Signature
DAVID ANDERSON
Branch Chief

William K. Vickery
Signature
WILLIAM K. VICKERY
Division Director

This report has been reviewed by the ESC Public Affairs Office (PA) and is releasable to the National Technical Information Service (NTIS).

Qualified requestors may obtain additional copies from the Defense Technical Information Center (DTIC). All others should apply to the National Technical Information Service (NTIS).

If your address has changed, if you wish to be removed from the mailing list, or if the addressee is no longer employed by your organization, please notify PL/TSI, 29 Randolph Road, Hanscom AFB, MA 01731-3010. This will assist us in maintaining a current mailing list.

Do not return copies of this report unless contractual obligation or notices on a specific document requires that it be returned.

REPORT DOCUMENTATION PAGE

Public reporting burden for this collection of information is estimated to average 1 hour per response, including the time for reviewing instructions, searching existing data sources, gathering and maintaining the data needed, and completing and reviewing the collection of information. Send comments regarding this burden estimate or any other aspect of this collection of information. including suggestions for reducing this burden, to Washington Headquarters Services, Directorate for Information Operations and Reports, 1215 Jefferson Davis Highway. Suite 1204, Arlington, VA 22202-4302, and to the Office of Management and Budget, Paperwork Reduction Project (0704-0188), Washington, DC 20503.

1. AGENCY USE ONLY (*Leave blank*)	2. REPORT DATE 18 August 1995	3. REPORT TYPE AND DATES COVERED Final Report (19 Jul 91 - 19 Jul 95)

4. TITLE AND SUBTITLE
DMSP Sensor Fusion Auroral E-layer Algorithm:
Functional Description

5. FUNDING NUMBERS
PE 35160F
PR DMSP TA 01 WU AC

6. AUTHOR(S)
Robert E. Daniell, Jr.

Contract F19628-91-C-0103

7. PERFORMING ORGANIZATION NAME(S) AND ADDRESS(ES)
Computational Physics, Inc.
Suite 202A
240 Bear Hill Road
Waltham, MA 02154

8. PERFORMING ORGANIZATION REPORT NUMBER

9. SPONSORING / MONITORING AGENCY NAME(S) AND ADDRESS(ES)
Phillips Laboratory
29 Randolph Road
Hanscom AFB, MA 01731-3010
Contract Manager: Christopher Sherman/GPIM

10. SPONSORING / MONITORING AGENCY REPORT NUMBER
PL-TR-95-2112

11. SUPPLEMENTARY NOTES

12A. DISTRIBUTION / AVAILABILITY STATEMENT

APPROVED FOR PUBLIC RELEASE;
DISTRIBUTION UNLIMITED

12b. DISTRIBUTION CODE

13. ABSTRACT (*Maximum 200 words*)

This report describes the DMSP Sensor Fusion algorithm for remote sensing of the Auroral E-layer using the SSUSI and SSJ/5 sensors to be flown on Block 5D DMSP satellites. It is a generalization of the SSUSI Single Sensor Auroral E-layer Algorithm described in an earlier report (PL-TR-94-2195) with many new capabilities. The algorithm analyzes SSJ/5 precipitating electron and ion data to characterize the precipitation parameters along the satellite track. It maps this information to the corresponding pixels of the SSUSI image and combines the SSJ/5 and SSUSI data to characterize the neutral composition along the satellite track. Using this information, the algorithm extrapolates the neutral composition information to off track pixels and uses this information as input to an improved single sensor algorithm. The data products provided by the algorithm include electron and ion precipitation characteristics (mean energy, energy flux), O to N2 and O2 to N2 ratios, and E-layer characteristics (peak density and height of the peak) for each pixel in the SSUSI image.

14. SUBJECT TERMS
auroral ionosphere, space environment, remote sensing, space weather, aurora, E-layer, thermospheric composition, auroral optical emissions

15. NUMBER OF PAGES
40

16. PRICE CODE

17. SECURITY CLASSIFICATION OF REPORT Unclassified	18. SECURITY CLASSIFICATION OF THIS PAGE Unclassified	19. SECURITY CLASSIFICATION OF ABSTRACT Unclassified	20. LIMITATION OF ABSTRACT SAR

Table of Contents

Accesion For		
NTIS CRA&I		☒
DTIC TAB		☐
Unannounced		☐
Justification _____		
By _____		
Distribution /		
Availability Codes		
Dist	Avail and / or Special	
A-1		

List of Illustrations

Executive Summary

The DMSP Sensor Fusion Auroral E-layer Algorithm builds on the methods used in the SSUSI single sensor algorithm, but makes use of information from the SSJ/5 sensor to improve the accuracy of the deduced E-layer parameters. The Algorithm operates in three stages: SSJ/5 data analysis, Sensor Fusion analysis of subsatellite SSUSI pixels, and SSUSI image analysis of off-track pixels. The SSJ/5 data analysis characterizes the precipitating electrons and protons along the satellite track. The Sensor fusion analysis combines the SSJ/5 data analysis with the optical intensities observed by SSUSI along the orbital track to deduce information on the neutral composition, in particular the ratio of column densities of atomic and molecular oxygen to the column density of molecular nitrogen. This information is extrapolated to the rest of the image where it is used along with the SSUSI image data to deduce the precipitation characteristics over the whole image. This information is then used to calculate the peak E-layer electron density and the height of the E-layer over the auroral portions of the image.

1. Introduction

The ability to monitor the auroral region has importance for satellite operations, communications, spacecraft tracking, and optical surveillance. The auroral region is characterized by the presence of strong fluxes of both electrons and ions with energies of several keV. These particles can collect on the surfaces of satellites and often have consequences for the operation of those satellites. These particles also produce auroral optical emissions that can interfere with ground based and satellite based optical surveillance systems. They also produce enhanced ionization in the E-layer and lower F-layer that may interfere with communications systems or with radar operations.

Auroral electrons and ions can be detected directly only by flying appropriate measurement devices through the precipitation region on satellites. To map the region even at a longitude resolution of 15° would require 24 satellites. Since it is not practical to operate more than two or three satellites at a time, mapping the precipitating particles must be done using remote sensing of the effects of the precipitating particles on the atmosphere.

Auroral optical emissions are produced by the impact of precipitating electrons and ions with energies of a few keV. The collisions of the electrons and ions with the constituents of the neutral atmosphere produce atoms and molecules in excited states. These excited atoms and molecules dispose of their excess energy by radiating at wavelengths ranging from infrared to X-rays.

Because the atmosphere is largely transparent to visible and infrared emissions, space based observations of auroral emissions at these wavelengths are plagued by albedo problems. Therefore, the ultraviolet (UV) wavelength range is preferable. The relationship between particle precipitation characteristics and UV emissions has been worked out using electron and proton transport models [*Strickland et al.*, 1983, 1984, 1993; *Daniell et al.*, 1985; *Daniell and Strickland*, 1986]. These papers also examined the influence of neutral atmosphere composition on the emissions and established the basic principles of deducing particle precipitation characteristics from UV measurements.

The single sensor SSUSI Auroral E-region algorithm (SSUSIAE) has been described in the interim Scientific Report No. 1 [*Daniell et al.*, 1994] for this contract. It characterizes electron and proton precipitation in the diffuse aurora using selected ultraviolet (UV) emissions produced in the E-region of the auroral ionosphere. SSUSIAE also calculates N_mE (the peak electron density of the E-region) and h_mE (the height of the E-region) based on the deduced particle precipitation characteristics. It is limited by the fact that the effects of neutral composition cannot be completely eliminated, introducing a large uncertainty in the deduced precipitation characteristics.

During the second half of this contract, we have generalized the approach used in the single sensor algorithm to incorporate data from the SSJ/5 instrument, which measures precipitating electrons and ions at the satellite. The incorporation of this data into the algorithm has several advantages. First, it permits better characterization of the precipitating particles.

1

Second, it permits the determination of neutral composition information. While this information is strictly available along the satellite track, it can be extrapolated to off track pixels with varying levels of confidence.

This report provides a functional description of the algorithm that contains sufficient detail to be the basis of a Language Independent Description from which a full implementation could be produced. However, it should be noted that only parts of the algorithm have actually been implemented, and others have not been defined in complete detail. This description should, therefore, be considered provisional.

2. Top Level Description

The algorithm consists of four major modules: (1) SSJ/5 data analysis, (2) subsatellite sensor fusion analysis, (3) off-track SSUSI image analysis, and (4) the Auroral E-layer analysis. The first three modules incorporate new analysis techniques that have not been included in previous sensor algorithms for these two instruments. The basic methods used in each module are described in the following subsections. The algorithm assumes that the dayglow and geocorona contributions have already been removed from the SSUSI images.

2.1 SSJ/5 Data Analysis

The first module, SSJ/5 data analysis, examines electron and ion spectra to determine the precipitation characteristics. For ions, this process is straightforward, since the ion spectra are usually well characterized by a Maxwellian (thermal) distribution with a characteristic energy of a few keV. The general form of a Maxwellian distribution is

$$f(E,\theta,\varphi)\sin\theta\,d\theta\,d\varphi\,dE = \frac{n}{2}\left(\frac{1}{\pi E_M}\right)^{\frac{1}{2}}\sqrt{E}\,\exp\left(-\frac{E}{E_M}\right)\sin\theta\,d\theta\,d\varphi\,dE \qquad (2.1)$$

where f is the number of particles with energy in the range E to $E+dE$ and velocity vector in the solid angle represented by the angular ranges θ to $\theta+d\theta$ and φ to $\varphi+d\varphi$. E_M is the characteristic energy (or temperature) of the distribution.

For a Maxwellian distribution, the differential flux of particles in a particular direction, denoted by the unit velocity vector $\hat{\mathbf{v}}$ is

$$\phi_N(E,\theta,\varphi)\sin\theta\,d\theta\,d\varphi\,dE = \frac{Q_M}{2\pi E_M^2}\,\hat{\mathbf{v}}\,\frac{E}{E_M}\,\exp\left[-\frac{E}{E_M}\right]\sin\theta\,d\theta\,d\varphi\,dE \qquad (2.2)$$

and the corresponding differential energy flux is

$$\phi_E(E,\theta,\varphi)\sin\theta\,d\theta\,d\varphi\,dE = \frac{Q_M}{2\pi E_M}\hat{\mathbf{v}}\left(\frac{E}{E_M}\right)^2\exp\left[-\frac{E}{E_M}\right]\sin\theta\,d\theta\,d\varphi\,dE \qquad (2.3$$

In these expressions, Q_M is the downward energy flux, obtained by integrating $\hat{\mathbf{z}}\cdot\phi_E$ over the downward hemisphere ($\frac{\pi}{2} < \theta \le \pi$, $0 \le \varphi < 2\pi$).

The shape of a Maxwellian distribution is completely determined by a single parameter, E_M. The peak of the number flux (the most probably energy) is E_M, the mean energy $\overline{E}_M$ is $2E_M$, while the full width at half maximum (FWHM) is ~2.91E_M. The peak of the energy flux is $2E_M$. The simplest way to analyze a Maxwellian spectrum is to divide the differential flux by E and to note that

$$\ln\left(\frac{1}{E}\phi_N\right) = \ln\left(\frac{Q_M}{2\pi E_M^3}\right) - \frac{E}{E_M} \qquad (2.4)$$

so that E_M is the inverse slope of the resulting straight line and Q_M may be obtained from the intercept. This is best done using the highest energy channels for which the measured flux is well above the instrument sensitivity. This reduces the chance of error due to the presence of a background of low energy particles.

For electrons, however, the spectrum is often a modifed Maxwellian. The usual modification is a shift to higher energies produced by parallel electric fields [*Hoffman*, 1993], although other modifications are possible. The electron data analysis distinguishes three cases (1) the diffuse aurora, characterized by a thermal (non-shifted) Maxwellian, (2) an inverted V event characterized by a shifted Maxwellian, and (3) a discrete arc characterized by nearly monoenergetic, field aligned beams that often deviate substantially from a simple Maxwellian shape.

The basic form of a shifted Maxwellian is

$$\phi_N^{(S)}(E,\theta,\varphi) = \begin{cases} \dfrac{Q_S}{2\pi\left(E_M^2 + E_S E_M + \frac{1}{2}E_S^2\right)}\hat{\mathbf{v}}\dfrac{E}{E_M}\exp\left[-\dfrac{E - E_S}{E_M}\right] & \text{for } E \ge E_S \\ 0 & \text{for } E < E_S \end{cases} \qquad (2.5)$$

As for the unmodified Maxwellian, the characteristic energy of the parent Maxwellian may be obtained from the inverse slope of the straight line $\ln\left(\frac{1}{E}\phi_N^{(S)}\right)$. However, the peak energy is no longer necessarily determined by the characteristic energy E_M. The peak of the spectrum is more pronounced in the energy flux, $\phi_E^{(S)} = E\phi_N^{(S)}$, where the peak occurs at $\max(E_M, E_S)$. Therefore, the electron analysis must determine whether the primary spectrum is shifted or not. Unshifted

3

Maxwellians are assumed to be isotropic over the downward hemisphere. Shifted Maxwellians are usually isotropic over most of the downward hemisphere.

Even after the primary spectrum has been characterized, the algorithm must check for a secondary peak somewhat less energetic than the primary peak. This peak is produced by degraded, backscattered primaries that are reflected by the accelerating potential [*Hoffman*, 1993]. These secondary peaks are usually nearly field aligned with pitch angles less than 30°. This is also true of at least some primary peaks in intense discrete arcs [*McFadden et al.*, 1990].

The electron data analysis assigns each electron spectrum (obtained once per second) to one of the three classes described above. Since the SSJ/5 instrument does not provide pitchangle information, a standard pitch angle distribution (different for each class) will be applied to each class. The downward electron energy flux (Q_{0e}) data and the characteristic electron energy (E_{0e}) will be used to assign a crude threshold for distinguishing diffuse aurora from inverted V and discrete arcs. These will be used in the SSUSI image analysis to assign an electron spectrum classification to each off track pixel.

2.2 The Sensor Fusion Analysis for subsatellite pixels

The algorithm must trace each spectrum along the spacecraft field line down to an altitude of 110 km and identify the pixel containing the foot of the field line. In most cases, more than one spectrum will be assigned to each pixel. The electron and ion spectral characteristics (as opposed to the electron and ion spectra themselves) will be averaged over the pixel, taking proper account not to blindly average different classes of spectra. The differential energy flux will be used to assign a dominant electron spectrum class to each pixel.

The electron and ion characteristics deduced from the SSJ/5 data analysis are used along with 121.6 nm, 135.6 nm, LBH1, and LBH2 yield curves to obtain the expected values of the intensities of those emission features using a nominal neutral atmosphere. The expected values are compared to the observed intensities to obtain values for the deviation of O/N_2 and O_2/N_2 ratios from their nominal values.

A boundary detection algorithm detects the equatorward and poleward edges of the aurora. Within the boundaries, a generalized coordinate, x, is defined. If the equatorward latitude is λ_{eq} and the poleward latitude is λ_p, then

$$x \equiv \frac{\lambda - \lambda_{eq}}{\lambda_p - \lambda_{eq}} \tag{2.6}$$

The O/N_2 and O_2/N_2 ratios are treated as functions of x. Generally, there will be two crossings of the auroral oval at two separate locat times by the same spacecraft. Let $f_0(x, T_1)$ be the O/N_2 ratio determined at the first local time and $f_0(x, T_2)$ be the ratio determined at the second locat time. Then the function at arbitrary local time T is

4

$$f(x,T) = a\cos\left(\frac{2\pi T}{24}\right) + b\sin\left(\frac{2\pi T}{24}\right) \tag{2.7}$$

where

$$a = \frac{f(x,T_1)\sin\left(\frac{2\pi T_2}{24}\right) - f(x,T_2)\sin\left(\frac{2\pi T_1}{24}\right)}{\cos\left(\frac{2\pi T_1}{24}\right)\sin\left(\frac{2\pi T_2}{24}\right) - \cos\left(\frac{2\pi T_2}{24}\right)\sin\left(\frac{2\pi T_1}{24}\right)}$$

$$b = \frac{f(x,T_2)\cos\left(\frac{2\pi T_1}{24}\right) - f(x,T_1)\cos\left(\frac{2\pi T_2}{24}\right)}{\cos\left(\frac{2\pi T_1}{24}\right)\sin\left(\frac{2\pi T_2}{24}\right) - \cos\left(\frac{2\pi T_2}{24}\right)\sin\left(\frac{2\pi T_1}{24}\right)}$$

The only requirement being that $T_1 \neq T_2$. A similar procedure is applied to the O_2/N_2 ratio, and the ion characteristic energy. (All ions are assumed to be protons.)

2.3 The SSUSI image data analysis.

For each pixel, the O/N_2 and O_2/N_2 ratios are determined by evaluating the appropriate function of the form given by Equation (2.7). The analysis now proceeds in two stages. In the first stage, the analysis assumes that both protons and electrons are present. Then there are four parameters (E_{0e}, Q_{0e}, E_{0p}, Q_{0p}) to be determined from four data elements (I_{1216}, I_{1356}, I_{LBH1}, I_{LBH2}).

In the first stage analysis, the electron spectrum is assumed to be Maxwellian. The four parameters and the four data elements are formally related by the four (nonlinear) equations

$$I_{1216} = Q_{0e}Y_{1216}^{(e)}\left(R_O, R_{O_2}; E_{0e}\right) + Q_{0p}Y_{1216}^{(p)}\left(R_O, R_{O_2}; E_{0p}\right) \tag{2.8a}$$

$$I_{1356} = Q_{0e}Y_{1356}^{(e)}\left(R_O, R_{O_2}; E_{0e}\right) + Q_{0p}Y_{1356}^{(p)}\left(R_O, R_{O_2}; E_{0p}\right) \tag{2.8b}$$

$$I_{LBH1} = Q_{0e}Y_{LBH1}^{(e)}\left(R_O, R_{O_2}; E_{0e}\right) + Q_{0p}Y_{LBH1}^{(p)}\left(R_O, R_{O_2}; E_{0p}\right) \tag{2.8c}$$

$$I_{LBH2} = Q_{0e}Y_{LBH2}^{(e)}\left(R_O, R_{O_2}; E_{0e}\right) + Q_{0p}Y_{LBH2}^{(p)}\left(R_O, R_{O_2}; E_{0p}\right) \tag{2.8d}$$

where the functions $Y_{1356}^{(e)}$ etc. represent the *yield* of the indicated emission from a downward energy flux of 1 erg cm^{-2} s^{-1} carried by the indicated particles. (Of course, $Y_{1216}^{(e)}$ vanishes identically.) R_O (R_{O_2}) is the scale factor for the atomic oxygen density (molecular oxygen density) from a model (e.g., MSIS-90) required to make the model give an O/N_2 (O_2/N_2) ratio

that conforms to the estimate extrapolated from the sensor fusion analysis. If R_O and R_{O_2} are known, then we have four (nonlinear) equations in four unknowns.

The Second Stage of the analysis depends on the results of the first stage analysis.

Case 1: If $0.05 \leq \dfrac{Q_{0e}}{Q_{0p}} \leq 20.0$ then both protons and electrons are present. Consider two cases:

    Case 1a: If $Q_{0e} \leq Q_{threshold}$ then the precipitation is probably due to the diffuse aurora, so Accept Stage 1 analysis without modification

    Case 1b: If $Q_{e0} > Q_{threshold}$ then the precipitation is probably due to an inverted V event or a discrete arc, so Redo Stage 1 analysis using monoenergetic electron yield functions rather than Maxwellian electron yield functions.

Case 2: If $\dfrac{Q_{0e}}{Q_{0p}} < 0.05$, then electrons are effectively absent. Therefore, perform Pure Proton analysis: 4 equations, 4 unknowns:

$$I_{1216} = Q_{0p} Y_{1216}^{(p)}\left(R_O, R_{O_2}; E_{0p}\right) \tag{2.9a}$$

$$I_{1356} = Q_{0p} Y_{1356}^{(p)}\left(R_O, R_{O_2}; E_{0p}\right) \tag{2.9b}$$

$$I_{\text{LBH1}} = Q_{0p} Y_{\text{LBH1}}^{(p)}\left(R_O, R_{O_2}; E_{0p}\right) \tag{2.9c}$$

$$I_{\text{LBH2}} = Q_{0p} Y_{\text{LBH2}}^{(p)}\left(R_O, R_{O_2}; E_{0p}\right) \tag{2.9d}$$

where the four unknowns are R_O, R_{O_2}, E_{0p}, and Q_{0p}.

Case 3: If $\dfrac{Q_{0e}}{Q_{0p}} > 20.0$, then protons are effectively absent. Therefore, perform Pure Electron analysis: 3 equations, 4 unknowns:

$$I_{1356} = Q_{0e} Y_{1356}^{(e)}\left(R_O, R_{O_2}; E_{0e}\right) \tag{2.10b}$$

$$I_{\text{LBH1}} = Q_{0e} Y_{\text{LBH1}}^{(e)}\left(R_O, R_{O_2}; E_{0e}\right) \tag{2.10c}$$

$$I_{\text{LBH2}} = Q_{0e} Y_{\text{LBH2}}^{(e)}\left(R_O, R_{O_2}; E_{0e}\right) \tag{2.10d}$$

One of the four unknowns, R_O, R_{O_2}, E_{0e}, and Q_{0e}, cannot be determined from the UV intensities alone. Since O_2 is likely to be less variable than O, the analysis assumes that R_{O_2} is given by Equation (2.7). The remaining three unknowns are now determined by Equations (2.10).

2.4 The Auroral E-layer Characteristics

The E-layer characteristics, $f_o E$ and $h_m E$, are determined in much the same way as in the single sensor algorithm, using an altitude dependent effective recombination coefficient. However, in the sensor fusion algorithm, the effective recombination coefficient will be a function of R_O and R_{O_2}.

3. SSJ/5 Data Analysis Module

This module ingests SSJ/5 data, analyses each ion and electron energy spectrum to determine the precipitation characteristics, E_{0p}, Q_{0p}, E_{0e}, Q_{0e}, S_e defined as

E_{0p} The characteristic (most probable or peak) energy in keV of the ions (assumed to be protons).

Q_{0p} The downward energy flux of the ions (erg cm^{-2} s^{-1})

E_{0e} The characteristic (most probable or peak) energy in keV of the main electron spectrum.

Q_{0e} The downward energy flux of the main electron spectrum (erg cm^{-2} s^{-1})

ST_e The spectral type of the main electron spectrum (Maxwellian, shifted Maxwellian, Monoenergetic).

SP_e A flag indicating the presence or absence of a secondary peak in the electron spectrum. If present, it is assumed to consist of degraded primaries, backscattered by the atmosphere and reflected by the auroral potential region.

E_{1e} The characteristic (most probable or peak) energy in keV of the secondary electron spectrum.

Q_{1e} The downward energy flux of the secondary electron spectrum (erg cm^{-2} s^{-1}).

The ions are assumed to always have a Maxwellian distribution. For the electrons, note that the "secondary electron spectrum" is different than the "spectrum of the secondary electrons."

3.1 SSJ/5 Data Ingestion and processing

The SSJ/5 data comes in the form of differential number fluxes of ions and electrons in 20 energy channels ranging from 30 eV to 30 keV. The channels are organized into two groups of 10. Channels 1 through 10 represent energies from 30 keV to 1 keV. Channels 11 through 20 represent energies from 1 keV to 30 eV. Channels 10 and 11 both measure 1 keV particles. Since the instrument steps through the two groups of channels in parallel, Channel 10 is counted at the end of the sweep while Channel 11 is counted at the beginning of the sweep. Consequently, the two measurements of 1 keV particles are often slightly different. A comparison of these two channels gives an indication of the amount of temporal aliasing present in the data.

A preprocessor for SSJ/4 data was provided for use with the PRISM algorithm. The PRISM preprocessor provides only mean energy (keV) and energy flux (erg cm^{-2} s^{-1}) The AEL Algorithm requires more extensive processing of the SSJ/5 data because it needs to distinguish between the diffuse aurora (characterized by broad, approximately Maxwellian, spectra) and discrete arcs (characterized by narrow spectra, often shifted Maxwellians). Therefore, the AEL Algorithm assumes the existence of a preprocessor for the SSJ/5 data whose output is the differential flux in each energy channel.

MODULE 1: SSJ/5 data ingestion

PURPOSE: To ingest preprocessed SSJ/5 data, correct for temporal aliasing, and reverse the energy ordering of the data.

INPUT:

$\varepsilon^{(e)} = \left[\varepsilon_1^{(e)}, \varepsilon_2^{(e)}, \ldots \varepsilon_{20}^{(e)}\right]$, **the vector of electron energy channels (eV)**

$\varepsilon^{(p)} = \left[\varepsilon_1^{(p)}, \varepsilon_2^{(p)}, \ldots \varepsilon_{20}^{(p)}\right]$, **the vector of ion energy channels (eV)**

$\mathbf{f}^{(e)} = \left[f_1^{(e)}, f_2^{(e)}, \ldots f_{20}^{(e)}\right]$, **the vector of electron differential particle fluxes (cm^{-2} s^{-1} eV^{-1} sr^{-1})**

$\mathbf{f}^{(p)} = \left[f_1^{(p)}, f_2^{(p)}, \ldots f_{20}^{(p)}\right]$, **the vector of ion differential particle fluxes (cm^{-2} s^{-1} eV^{-1} sr^{-1})**

$\mathbf{s}^{(e)} = \left[s_1^{(e)}, s_2^{(e)}, \ldots s_{20}^{(e)}\right]$, **the vector of electron channel sensitivities, i.e., the differential electron flux corresponding to 1 count**

$\mathbf{s}^{(p)} = \left[s_1^{(p)}, s_2^{(p)}, \ldots s_{20}^{(p)}\right]$, **the vector of ion channel sensitivities, i.e., the differential ion flux corresponding to 1 count**

NOTE: For both electrons and ions $\varepsilon_1 > \varepsilon_2 > \ldots \varepsilon_{10}$ and $\varepsilon_{11} > \varepsilon_{12} > \ldots \varepsilon_{20}$. ε_{10} and ε_{11} are both approximately 1000 eV, but no special ordering of these two energies is assumed.

OUTPUT:

$\mathbf{E}^{(e)} = \left[E_1^{(e)}, E_2^{(e)}, \ldots E_{19}^{(e)}\right]$, **the vector of electron channel energies with $E_{n+1}^{(e)} > E_n^{(e)}$**

$\phi^{(e)} = \left[\phi_1^{(e)}, \phi_2^{(e)}, \ldots \phi_{19}^{(e)}\right]$, **the corresponding vector of electron channel fluxes (cm^{-2} s^{-1} eV^{-1} sr^{-1}).**

$\mathbf{E}^{(p)} = \left[E_1^{(p)}, E_2^{(p)}, \ldots E_{19}^{(p)}\right]$, **the vector of ion channel energies with $E_{n+1}^{(p)} > E_n^{(p)}$**

$\phi^{(p)} = \left[\phi_1^{(p)}, \phi_2^{(p)}, \ldots \phi_{19}^{(p)}\right]$, **the corresponding vector of ion channel fluxes (cm^{-2} s^{-1} eV^{-1} sr^{-1}).**

$\mathbf{S}^{(e)} = \left[S_1^{(e)}, S_2^{(e)}, \ldots S_{19}^{(e)}\right]$, **the vector of electron channel sensitivities, i.e., the differential electron flux corresponding to 1 count**

$\mathbf{S}^{(p)} = \left[S_1^{(p)}, S_2^{(p)}, \ldots S_{19}^{(p)}\right]$, **the vector of ion channel sensitivities, i.e., the differential ion flux corresponding to 1 count**

NOTE: For both electrons and ions, the ordering of the energy channels has been reversed relative to the input convention, and one of the redundant 1 keV channels has been removed.

Step 1: Interpolate channels 10 and 11 to precisely 1 keV.

Definition: $F_{10}^{(e)}$ is the 1 keV electron flux inferred from the channel 10 flux, $f_{10}^{(e)}$

Definition: $F_{11}^{(e)}$ is the 1 keV electron flux inferred from the channel 11 flux, $f_{11}^{(e)}$

Definition: $F_{10}^{(p)}$ is the 1 keV proton flux inferred from the channel 10 flux, $f_{10}^{(p)}$

Definition: $F_{11}^{(p)}$ is the 1 keV proton flux inferred from the channel 11 flux, $f_{11}^{(p)}$

$$F_{10}^{(e)} = \exp\left[\ln f_{10}^{(e)} + \frac{1000 - \varepsilon_{10}^{(e)}}{\varepsilon_9^{(e)} - \varepsilon_{10}^{(e)}}\left(\ln f_9^{(e)} - \ln f_{10}^{(e)}\right)\right]$$

$$F_{11}^{(e)} = \exp\left[\ln f_{11}^{(e)} + \frac{1000 - \varepsilon_{11}^{(e)}}{\varepsilon_{12}^{(e)} - \varepsilon_{11}^{(e)}}\left(\ln f_{12}^{(e)} - \ln f_{11}^{(e)}\right)\right]$$

$$F_{10}^{(p)} = \exp\left[\ln f_{10}^{(p)} + \frac{1000 - \varepsilon_{10}^{(p)}}{\varepsilon_9^{(p)} - \varepsilon_{10}^{(p)}}\left(\ln f_9^{(p)} - \ln f_{10}^{(p)}\right)\right]$$

$$F_{11}^{(p)} = \exp\left[\ln f_{11}^{(p)} + \frac{1000 - \varepsilon_{11}^{(p)}}{\varepsilon_{12}^{(p)} - \varepsilon_{11}^{(p)}}\left(\ln f_{12}^{(p)} - \ln f_{11}^{(p)}\right)\right]$$

Step 2: Determine the change in 1 keV flux over the duration of the sweep:

$$\Delta F^{(e)} = F_{10}^{(e)} - F_{11}^{(e)}$$
$$\Delta F^{(p)} = F_{10}^{(p)} - F_{11}^{(p)}$$

Step 3: Refer each channel's flux back to the start of the sweep:

For $i = 1,2,...9$ do

$\quad j = 20 - i$

$$\phi_j^{(e)} = \left[1 - \frac{i-1}{9}\frac{\Delta F^{(e)}}{F_{10}^{(e)}}\right]f_i^{(e)}$$

$$\phi_j^{(p)} = \left[1 - \frac{i-1}{9}\frac{\Delta F^{(p)}}{F_{10}^{(p)}}\right]f_i^{(p)}$$

$$E_j^{(e)} = \varepsilon_i^{(e)}$$
$$E_j^{(p)} = \varepsilon_i^{(p)}$$
$$S_j^{(e)} = s_i^{(e)}$$
$$S_j^{(p)} = s_i^{(p)}$$

End do
$$\phi_{10}^{(e)} = f_{11}^{(e)}$$
$$\phi_{10}^{(p)} = f_{11}^{(p)}$$
$$E_{10}^{(e)} = \varepsilon_{11}^{(e)}$$
$$E_{10}^{(p)} = \varepsilon_{11}^{(p)}$$
$$S_{10}^{(e)} = s_{11}^{(e)}$$
$$S_{10}^{(p)} = s_{11}^{(p)}$$

For $i = 11, 12, \ldots 19$ do
$$j = 20 - i$$
$$\phi_j^{(e)} = \left[1 - \frac{i-10}{9}\frac{\Delta F^{(e)}}{F_{10}^{(e)}}\right]f_{i+1}^{(e)}$$
$$\phi_j^{(p)} = \left[1 - \frac{i-10}{9}\frac{\Delta F^{(p)}}{F_{10}^{(p)}}\right]f_{i+1}^{(p)}$$
$$E_j^{(e)} = \varepsilon_{i+1}^{(e)}$$
$$E_j^{(p)} = \varepsilon_{i+1}^{(p)}$$
$$S_j^{(e)} = s_{i+1}^{(e)}$$
$$S_j^{(p)} = s_{i+1}^{(p)}$$
End do
END MODULE 1.

3.2 Electron data analysis

Electron and ion data are analyzed separately because the two types of auroral particles are subject to different physical processes. The algorithm recognizes three types of electron spectra: Maxwellian, Shifted Maxwellian, and Monoenergetic. (Technically, shifted Maxwellians are a kind of monoenergetic spectrum.)

Maxwellian spectra are characteristic of the diffuse aurora, which is produced by a population of (hot) thermal electrons. Such a spectrum is broad and isotropic. It is often accompanied by a low energy component consisting of secondary electrons. This low energy component has little effect on the auroral E-layer/

Shifted Maxwellian spectra a characteristic of inverted-V events and consist of thermal electrons that have been accelerated (and sometimes heated) by passage through a field-aligned potential drop. The spectral shape is still Maxwellian, but the peak energy is much higher than the characteristic energy of the Maxwellian. Since the width of the spectrum is no much smaller than the peak energy, the spectrum appears to be nearly monoenergetic. The spectrum is usually nearly isotropic. A secondary peak in the spectrum is often present. This secondary peak consists of degraded primaries that are backscattered up the magnetic field line but are reflected by the auroral potential region. The secondary peak is nearly field aligned.

Monoenergetic spectra a characteristic of discrete arcs and other auroral features in which the Maxwellian shape of the parent population of electrons is sufficiently distorted so that a Maxwellian based analysis is not possible. A secondary peak and other confounding structure may or may not be present.

10

MODULE 2: SSJ/5 electron data analysis

PURPOSE: To determine whether the electron spectrum may be characterized as Maxwellian, shifted Maxwellian, or monoenergetic, and to determine the characteristics of the main and (if present) secondary peaks.

INPUT:

$\mathbf{E}^{(e)} = \left[E_1^{(e)}, E_2^{(e)}, \ldots E_{19}^{(e)} \right]$, **the vector of electron channel energies (eV) with** $E_{n+1}^{(e)} > E_n^{(e)}$

$\phi^{(e)} = \left[\phi_1^{(e)}, \phi_2^{(e)}, \ldots \phi_{19}^{(e)} \right]$, **the corresponding vector of electron channel fluxes (cm^{-2} s^{-1} eV^{-1} sr^{-1}).**

$\mathbf{S}^{(e)} = \left[S_1^{(e)}, S_2^{(e)}, \ldots S_{19}^{(e)} \right]$, **the corresponding channel sensitivity, i.e., the flux corresponding to 1 count.**

OUTPUT:

ST_e, **a string variable containing "Maxwellian" if the electron flux appears to be an unshifted Maxwellian, or "Shifted Maxwellian" if the electron flux appears to be a shifted Maxwellian, or "Monoenergetic" if the electron flux appears to be a narrow peak of uncertain or non-Maxwellian shape.**

E_{0e}, **the characteristic (maximum or most probable) energy (keV) of the main peak of the electron spectrum.**

Q_{0e}, **the downward energy flux (erg cm^{-2} s^{-1}) of the main peak of the electron spectrum.**

E_{MS}, **the characteristic energy of the parent Maxwellian when the electron spectrum is identified as a "Shifted Maxwellian." For "Maxwellian" or "Monoenergetic" spectra, this variable is exactly 0.**

SP_e, **a logical variable with the value TRUE if a secondary electron peak is detected, and the value FALSE otherwise.**

E_{1e}, **the characteristic energy (keV) of the secondary peak (if any) of the electron spectrum. If SECONDARY is FALSE, this variable is undefined.**

Q_{1e}, **the downward energy flux (erg cm^{-2} s^{-1}) of the secondary peak (if any) of the electron spectrum. If SECONDARY is FALSE, this variable is undefined.**

W_{1e}, **the full width at half maximum (FWHM) of the secondary peak (if any) of the electron spectrum. If SECONDARY is FALSE, this variable is undefined.**

Begin Procedure

Step 1. Locate the absolute maximum in the *energy flux* spectrum:

Definition: $\psi^{(e)}$ is a vector containing the energy flux spectrum (eV cm^{-2} s^{-1} sr^{-1}).

Definition: j_{max} is the subscript or index (channel number) of the maximum element of $\psi^{(e)}$

Definition: ψ_{max} is the value of the maximum element of $\psi^{(e)}$ (eV cm^{-2} s^{-1} sr^{-1}).

Definition: E_{max} is the energy (eV) of channel j_{max}

11

Definition: MAX is a function procedure or module that accepts as input a vector of numerical values and returns the largest of these along with it subscript.

$$\psi^{(e)} = \left[E_1^{(e)} \phi_1^{(e)}, E_2^{(e)} \phi_2^{(e)}, \dots E_{19}^{(e)} \phi_{19}^{(e)} \right]$$

$$\psi_{max} = MAX\left(\psi^{(e)}, j_{max} \right)$$

$$E_{max} = E_{j_{max}}^{(e)}$$

Step 2. Determine the characteristics of the primary spectrum.

Definition: $\eta^{(e)}$ is the phase space flux density

Definition: LLSQ is a procedure or module that accepts a vector of x values and a vector of y values and performs a linear least square fit of the function $ax + b$ to those values.

Definition: N_{fit} is the number of points from the electron spectrum to be used in LLSQ

Definition: E_M is the characteristic energy (eV) of a Maxwellian energy spectrum.

Definition: E_S is the energy shift (eV) of a Shifted Maxwellian energy spectrum.

Definition: Q_M is the downward energy flux (eV cm^{-2} s^{-1}) of a Maxwellian energy spectrum that is isotropic over the downward hemisphere

$j_{stop} = 19$

$j = j_{max} + 1$

While $j_{stop} = 19$ do

    If $\phi_j^{(e)} \leq S_j^{(e)}$ Then

        $j_{stop} = j - 1$

    End If

    $j = j + 1$

End While

If $j_{stop} \leq j_{max} + 1$ Then

    The spectrum cannot be analyzed in terms of Maxwellians

Else

    $N_{fit} = j_{stop} - j_{max}$

End IF

$$\eta^{(e)} = \left[\frac{\phi_1^{(e)}}{E_1^{(e)}}, \frac{\phi_2^{(e)}}{E_2^{(e)}}, \dots \frac{\phi_{19}^{(e)}}{E_{19}^{(e)}} \right]$$

If $N_{fit} = 2$ Then

    The two points define a straight line:

12

$$a = \frac{\ln \eta^{(e)}_{j_{max}+2} - \ln \eta^{(e)}_{j_{max}+1}}{E^{(e)}_{j_{max}+2} - E^{(e)}_{j_{max}+1}}$$

$$b = \frac{E^{(e)}_{j_{max}+2} \eta^{(e)}_{j_{max}+1} - E^{(e)}_{j_{max}+1} \eta^{(e)}_{j_{max}+2}}{E^{(e)}_{j_{max}+2} - E^{(e)}_{j_{max}+1}}$$

Else

    Use LLSQ

$$\mathbf{y} = \left[\ln \eta^{(e)}_{j_{max}+1}, \ln \eta^{(e)}_{j_{max}+2}, \ldots \ln \eta^{(e)}_{j_{stop}}\right]$$

$$\mathbf{x} = \left[E^{(e)}_{j_{max}+1}, E^{(e)}_{j_{max}+2}, \ldots E^{(e)}_{j_{stop}}\right]$$

$$\text{LLSQ}\left(N_{fit}, \mathbf{x}, \mathbf{y}, a, b\right)$$

End If

$$E_M = -\frac{1}{a}$$

NOTE: For a Maxwellian, the peak of the energy flux occurs at twice the characteristic energy. Thus, we expect $E_M \approx \frac{1}{2} E_{max}$ for an unshifted Maxwellian. If this condition holds, then we classify the spectrum as diffuse aurora. If $E_M << E^{(e)}_{j_{max}}$, then we classify the spectrum as a discrete arc.

$$\delta E_{max} = 2 E_M - E_{max}$$
$$\Delta_{low} = E^{(e)}_{j_{max}} - E^{(e)}_{j_{max}-1}$$
$$\Delta_{high} = E^{(e)}_{j_{max}+1} - E^{(e)}_{j_{max}}$$

If $\delta E_{max} \leq 0$ Then

    If $\left|\delta E_{max}\right| \leq \Delta_{low}$ Then

        The data are consistent with a Maxwellian energy spectrum

        $ST_e = $ "Maxwellian"

        $E_{0e} = 10^{-3} E_M$

        $Q_M = 2\pi E_M^2 e^b$

        $Q_{0e} = 1.6 \times 10^{-12} Q_M$

    Else

        The data are consistent with a shifted Maxwellian energy spectrum

        $ST_e = $ "Shifted Maxwellian"

        $E_S = E_{max}$

        $E_{0e} = 10^{-3} E_{max}$

        $E_{MS} = 10^{-3} E_M$

$$Q_M = 2\pi \left(E_M^2 + E_M E_S + \tfrac{1}{2} E_S^2\right) E_M \exp\left(b - \frac{E_S}{E_M}\right)$$

        $Q_{0e} = 1.6 \times 10^{-12} \times Q_M$

End If

Else If $\delta E_{max} > 0$ Then

    If $\delta E_{max} \leq \Delta_{high}$ Then

        The data are consistent with a Maxwellian energy spectrum

        $ST_e = $ "Maxwellian"

        $E_{0e} = 10^{-3} E_M$

        $Q_M = 2\pi E_M^2 e^b$

        $Q_{0e} = 1.6 \times 10^{-12} Q_M$

    Else

        The data are not consistent with either a Maxwellian or a Shifted Maxwellian energy spectrum.

        Details are TBD.

    End If

End If

Step 3. Model the primary spectrum according to the characteristics determined in Step 2.

Definition: $\Phi^{(e)}$ is the model primary electron spectrum based on the characteristics determined in Step 2.

Definition: MXW is a function procedure that calculates the differential number flux of a (possible shifted) Maxwellian given Q_M, E_M, and E_S:

$$\text{MXW}(E, Q_M, E_M, E_S) \equiv \begin{cases} \dfrac{Q_M}{2\pi\left(E_M^2 + E_M E_S + \frac{1}{2} E_S^2\right)} \dfrac{E}{E_M} \exp\left(-\dfrac{E - E_S}{E_M}\right), & E \geq E_S \\ 0 & E < E_S \end{cases}$$

Definition: Φ_{max} is the maximum value of the model flux:

$$\Phi_{max} \equiv \begin{cases} \text{MXW}(E_M, Q_M, E_M, E_S), & E_M \geq E_S \\ \text{MXW}(E_S, Q_M, E_M, E_S), & E_M < E_S \end{cases}$$

Definition: E_{0max} is the energy corresponding to Φ_{max}

$$\Phi^{(e)} = \left[\text{MXW}\left(E_1^{(e)}, Q_M, E_M, E_S\right), \text{MXW}\left(E_2^{(e)}, Q_M, E_M, E_S\right), \dots \text{MXW}\left(E_{19}^{(e)}, Q_M, E_M, E_S\right)\right]$$

If $E_S \leq E_M$ Then

$$\Phi_{max} = \frac{Q_M}{2\pi\left(E_M^2 + E_M E_S + \frac{1}{2} E_S^2\right)} \exp\left(\frac{E_S}{E_M} - 1\right)$$

    $E_{0max} = E_M$

Else

$$\Phi_{max} = \frac{Q_M}{2\pi\left(E_M^2 + E_M E_S + \frac{1}{2} E_S^2\right)} \frac{E_S}{E_M}$$

End If

Step 4. Determine the characteristics of the secondary peak (if it is present).

Definition: $\xi^{(e)}$ is the measured differential electron spectrum after subtraction of the modeled primary spectrum from Step 3.

Definition: ξ_{max} is the maximum element of $\xi^{(e)}$

Definition: k_{max} is the subscript or index of ξ_{max}

Definition: E_1 is the energy of channel k_{max}

Definition: ω_{max} is the differential energy flux at E_1

$$\xi^{(e)} = \left[MAX\left(\phi_1^{(e)} - \Phi_1^{(e)}, 0\right), MAX\left(\phi_2^{(e)} - \Phi_2^{(e)}, 0\right), \dots MAX\left(\phi_{19}^{(e)} - \Phi_{19}^{(e)}, 0\right) \right]$$

$$\xi_{max} = MAX\left(\xi^{(e)}, k_{max}\right)$$

$$E_1 = E_{k_{max}}^{(e)}$$

$$\omega_{max} = E_1 \xi_{max}$$

If $\omega_{max} < 10^{-2} E_{0max} \Phi_{max}$ Then

    The flux in the secondary peak is too small to matter

$$E_{1e} = \tfrac{1}{2} E_{0e}$$

$$Q_{1e} = 0$$

$$W_{1e} = \tfrac{1}{5} E_{1e}$$

Else

    The flux in the secondary peak should not be neglected

    Find FWHM - details TBD.

End If

END MODULE 2.

3.3 Proton data analysis

Electron and ion data are analyzed separately because the two types of auroral particles are subject to different physical processes. The proton algorithm assumes that the energy spectrum is approximately Maxwellian.

MODULE 3: SSJ/5 proton data analysis

PURPOSE: To determine the characteristics of the proton energy spectrum.

INPUT:

    $\mathbf{E}^{(p)} = \left[E_1^{(p)}, E_2^{(p)}, \dots E_{19}^{(p)} \right]$, **the vector of proton channel energies (eV) with** $E_{n+1}^{(p)} > E_n^{(p)}$

    $\phi^{(p)} = \left[\phi_1^{(p)}, \phi_2^{(p)}, \dots \phi_{19}^{(p)} \right]$, **the corresponding vector of proton channel fluxes (cm^{-2} s^{-1} eV^{-1} sr^{-1}).**

$\mathbf{S}^{(p)} = \left[S_1^{(p)}, S_2^{(p)}, \dots S_{19}^{(p)} \right]$, **the corresponding channel sensitivity, i.e., the flux**

corresponding to 1 count.

OUTPUT:

E_{0p}, **the characteristic (maximum or most probable) energy (keV) of the main peak of the proton spectrum.**

Q_{0p}, **the downward energy flux (erg cm^{-2} s^{-1}) of the main peak of the proton spectrum.**

Begin Procedure

Step 1. Locate the absolute maximum in the *energy flux* spectrum:

Definition: $\psi^{(p)}$ is a vector containing the energy flux spectrum (eV cm^{-2} s^{-1} sr^{-1}).

Definition: j_{max} is the subscript or index (channel number) of the maximum element of $\psi^{(p)}$

Definition: ψ_{max} is the value of the maximum element of $\psi^{(p)}$ (eV cm^{-2} s^{-1} sr^{-1}).

Definition: E_{max} is the energy (eV) of channel j_{max}

Definition: MAX is a function procedure or module that accepts as input a vector of numerical values and returns the largest of these along with it subscript.

$$\psi^{(p)} = \left[E_1^{(p)} \phi_1^{(p)}, E_2^{(p)} \phi_2^{(p)}, \dots E_{19}^{(p)} \phi_{19}^{(p)} \right]$$
$$\psi_{max} = \mathrm{MAX}\left(\psi^{(p)}, j_{max} \right)$$
$$E_{max} = E_{j_{max}}^{(p)}$$

Step 2. Determine the characteristics of the proton spectrum.

Definition: $\eta^{(p)}$ is the phase space flux density

Definition: LLSQ is a procedure or module that accepts a vector of x values and a vector of y values and performs a linear least square fit of the function $ax + b$ to those values.

Definition: N_{fit} is the number of points from the proton spectrum to be used in LLSQ

Definition: E_M is the characteristic energy (eV) of a Maxwellian energy spectrum.

Definition: Q_M is the downward energy flux (eV cm^{-2} s^{-1}) of a Maxwellian energy spectrum that is isotropic over the downward hemisphere

$j_{stop} = 19$
$j = j_{max} + 1$
While $j_{stop} = 19$ do
    If $\phi_j^{(p)} \le S_j^{(p)}$ Then
        $j_{stop} = j - 1$

16

End If
$$j = j + 1$$
End While
If $j_{stop} \leq j_{max} + 1$ Then
The spectrum cannot be analyzed in terms of Maxwellians
Else
$$N_{fit} = j_{stop} - j_{max}$$
End IF

$$\eta^{(p)} = \left[\frac{\phi_1^{(p)}}{E_1^{(p)}}, \frac{\phi_2^{(p)}}{E_2^{(p)}}, \cdots \frac{\phi_{19}^{(p)}}{E_{19}^{(p)}} \right]$$

If $N_{fit} = 2$ Then
The two points define a straight line:
$$a = \frac{\ln \eta_{j_{max}+2}^{(p)} - \ln \eta_{j_{max}+1}^{(p)}}{E_{j_{max}+2}^{(p)} - E_{j_{max}+1}^{(p)}}$$
$$b = \frac{E_{j_{max}+2}^{(p)} \eta_{j_{max}+1}^{(p)} - E_{j_{max}+1}^{(p)} \eta_{j_{max}+2}^{(p)}}{E_{j_{max}+2}^{(p)} - E_{j_{max}+1}^{(p)}}$$
Else
Use LLSQ
$$\mathbf{y} = \left[\ln \eta_{j_{max}+1}^{(p)}, \ln \eta_{j_{max}+2}^{(p)}, \ldots \ln \eta_{j_{stop}}^{(p)} \right]$$
$$\mathbf{x} = \left[E_{j_{max}+1}^{(p)}, E_{j_{max}+2}^{(p)}, \ldots E_{j_{stop}}^{(p)} \right]$$
$$\text{LLSQ}\left(N_{fit}, \mathbf{x}, \mathbf{y}, a, b \right)$$
End If

$$E_M = -\frac{1}{a}$$

NOTE: For a Maxwellian, the peak of the energy flux occurs at twice the characteristic energy. Thus, we expect $E_M \approx \frac{1}{2} E_{max}$ for an unshifted Maxwellian.

$$\delta E_{max} = 2 E_M - E_{max}$$
$$\Delta_{low} = E_{j_{max}}^{(p)} - E_{j_{max}-1}^{(p)}$$
$$\Delta_{high} = E_{j_{max}+1}^{(p)} - E_{j_{max}}^{(p)}$$
If $\delta E_{max} \leq 0$ Then
    If $\left| \delta E_{max} \right| \leq \Delta_{low}$ Then
        The data are consistent with a Maxwellian energy spectrum
        $$E_{0p} = 10^{-3} E_M$$
        $$Q_M = 2\pi E_M^2 e^b$$

17

$$Q_{0p} = 1.6 \times 10^{-12} Q_M$$

Else

        The data are not consistent with a shifted Maxwellian energy spectrum

        Return Error Condition TBD.

    End If

Else If $\delta E_{max} > 0$ Then

    If $\delta E_{max} \leq \Delta_{high}$ Then

        The data are consistent with a Maxwellian energy spectrum

$$E_{0p} = 10^{-3} E_M$$
$$Q_M = 2\pi E_M^2 e^b$$
$$Q_{0p} = 1.6 \times 10^{-12} Q_M$$

    Else

        The data are not consistent with a Maxwellian energy spectrum.

        Return Error Condition TBD.

    End If

End If

END MODULE 3.

---

4. SSUSI On-Track Data Analysis Module

This module ingests SSUSI 121.6 nm, 135.6 nm, LBH1, and LBH2 images, identifies the pixels that lie on the DMSP orbital track, and analyses the image data in conjunction with the SSJ/4 data (sensor fusion). The SSUSI data is assumed to consist of intensities (Rayleighs) associated with each pixel. The dayglow and geocoronal backgrounds are assumed to have been subtracted, leaving only the auroral contribution. Each pixel is assumed to be associated with a geographic location (latitude, longitude), geomagnetic location, and solar zenith angle. The notation used in this section includes

I_{1216}:   The 121.6 nm (Lyman alpha) intensity due to proton precipitation. (R)

I_{1356}:   The 135.6 nm intensity due to electron and ion precipitation (R)

I_{LBH1}:   The LBH1 (140-150 nm) intensity due to electron and ion precipitation (R)

I_{LBH2}:   The LBH2 (165-180 nm) intensity due to electron and ion precipitation (R)

λ_g: The geographic latitude of the pixel (deg)

φ_g: The geographic longitude (deg)

λ_m: The geomagnetic latitude (deg)

φ_m: The geomagnetic longitude (deg)

χ: The solar zenith angle (deg)

τ: Universal Time (UT, hours)

T_s: Solar Local Time (SLT, hours)

18

T_m: Magnetic Local Time (MLT, hours)

4.1 SSUSI Data Ingestion and processing

The SSJ/5 data comes in the form of intensities in four wavelength channels. The intensities are in Rayleighs (R).

I_{1216} is the intensity of the Lyman alpha line of atomic hydrogen at 122 nm. The auroral component comes exclusively from precipitating protons and hydrogen atoms. There is no electron component.

I_{1356} is the combined intensity of the atomic oxygen $2p^4\ ^3P - 3s\ ^5S$ transition at 136 nm and the (3,0) band at 135 nm of the Lyman-Birge-Hopfield system of molecular Nitrogen. Both protons and electrons may contribute to the observed intensity.

I_{LBH1} is the intensity of all of the LBH bands in the 140-150 nm channel, along with the atomic nitrogen $2p^3\ ^2D - 3s\ ^2P$ transition at 149 nm. Both protons and electrons may contribute to the observed intensity.

I_{LBH2} is the intensity of all of the LBH bands in the 165-180 nm channel, along with the atomic nitrogen $2p^3\ ^2P - 3s\ ^2P$ transition at 174 nm. Both protons and electrons may contribute to the observed intensity.

MODULE 1: SSUSI data ingestion

PURPOSE: To ingest preprocessed SSUSI image data. The precise definition of this module depends on the precise way in which it is to interact with the SSUSI single sensor algorithm.

INPUT:
The location of the SSUSI image data.

NOTE: The information required to specify the location of the SSUSI data depends on the details of the SSUSI single sensor algorithm.

OUTPUT:
n_x, the number of pixels in the cross-track direction
n_y, the number of pixels in the along-track direction
I_{1216}, an n_x by n_y dimensional array containing the 121.6 nm intensity I_{1216} for each of the $n_x \times n_y$ pixels

$\mathbf{I}_{1356}$, an n_x by n_y dimensional array containing the 135.6 nm intensity I_{1356} for each of the $n_x \times n_y$ pixels

$\mathbf{I}_{LBH1}$, an n_x by n_y dimensional array containing the LBH1 intensity I_{LBH1} for each of the $n_x \times n_y$ pixels

$\mathbf{I}_{LBH2}$, an n_x by n_y dimensional array containing the LBH2 intensity I_{LBH2} for each of the $n_x \times n_y$ pixels

$\mathbf{G}$, an n_x by n_y dimensional array containing the geographic coordinates for each of the $n_x \times n_y$ pixels. Each element of the array consists of a latitude-longitude pair $\left(\lambda_g, \varphi_g\right)$.

$\mathbf{M}$, an n_x by n_y dimensional array containing the geomagnetic coordinates for each of the $n_x \times n_y$ pixels. Each element of the array consists of a latitude-longitude pair $\left(\lambda_m, \varphi_m\right)$.

χ, an n_x by n_y dimensional array containing the solar zenith angle χ for each of the $n_x \times n_y$ pixels.

ψ, an n_x by n_y dimensional array containing the nadir angle ψ for each of the $n_x \times n_y$ pixels.

NOTE: Individual elements of the above arrays will be denoted by a symbol of the form $\mathbf{A}(m,n)$ where $\mathbf{A}$ is an n_x by n_y array, m represents the column and n the row of the particular pixel. See Figure 1 for an illustration.

Step 1: Access image data, reformat as necessary, store in output arrays. Details TBD.
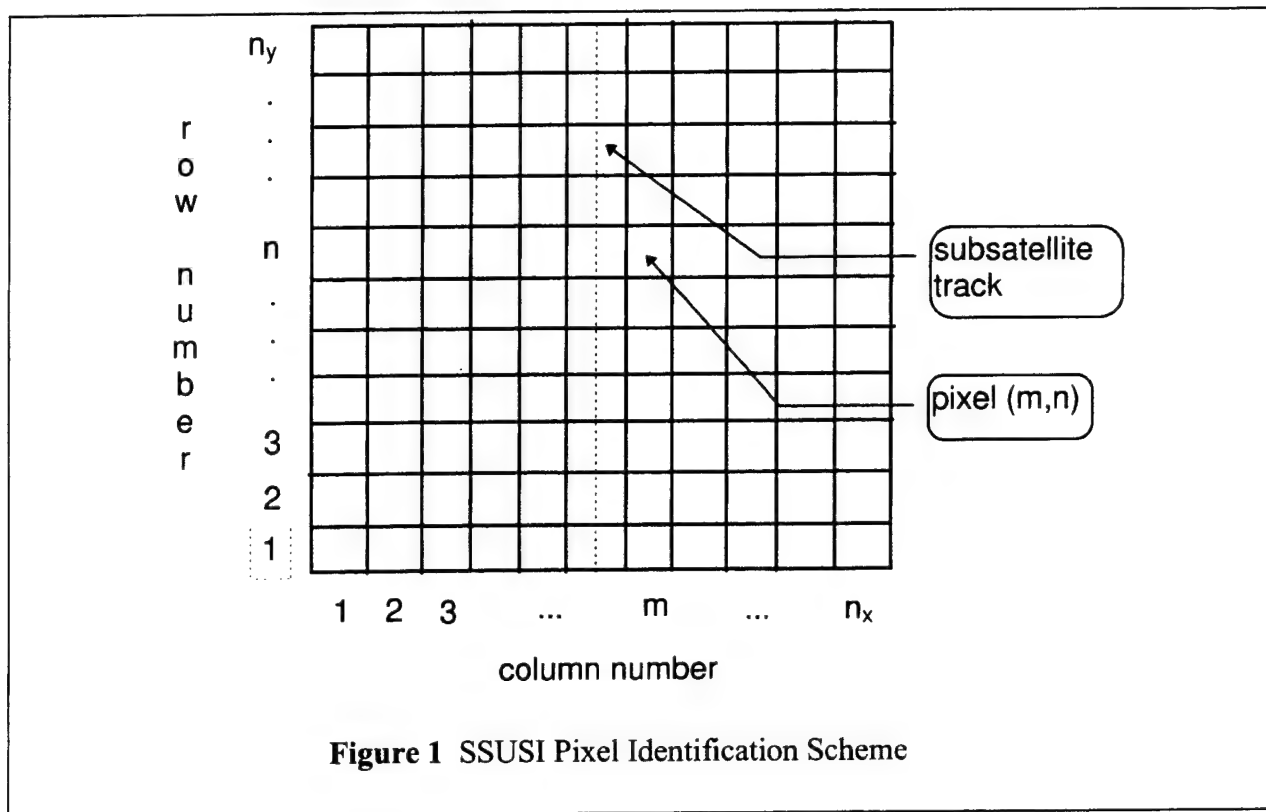
END MODULE 1.

Figure 1 SSUSI Pixel Identification Scheme

4.2 Identification of subsatellite pixels

The electrons and ions measured by the SSJ/5 instrument are guided by field lines and deposit their energy in the atmosphere threaded by the field line passing through the satellite at the time of the measurement. Thus, for the purposes of this algorithm, "subsatellite" does not indicate the pixel directly beneath the satellite, but the pixel through which the satellite's field line passes. The algorithm assumes that the emitting layer is at 110 km, so it traces the field line down from the satellite altitude to that altitude to determine through which pixel it passes.

MODULE 2: Identification of subsatellite pixels

PURPOSE: To trace field lines from the satellite to the E-layer, nominally 110 km, and to identify subsatellite pixels. Note that these will not necessarily be pixels along the central column of the image because the algorithm defines subsatellite as lying on the same field line as the satellite but at an altitude of 110 km. Since there will generally be more than one spectra corresponding to the same pixel, the module produces an "average" set of spectral characteristics for each subsatellite pixel.

INPUT:

N_s, the number of electron and/or ion spectra taken during the same time interval as the image

$\tau = \left[\tau_1, \tau_2, ... \tau_{N_s} \right]$, the vector of times (UT) corresponding to each of the N_s spectra

$\lambda = \left[\lambda_1, \lambda_2, ... \lambda_{N_s} \right]$, the vector of satellite geographic latitudes corresponding to each of the N_s spectra

$\varphi = \left[\varphi_1, \varphi_2, ... \varphi_{N_s} \right]$, the vector of satellite geographic longitudes corresponding to each of the N_s spectra

$\mathbf{h} = \left[h_1, h_2, ... h_{N_s} \right]$, the vector of satellite altitudes corresponding to each of the N_s spectra

G, an n_x by n_y dimensional array containing the geographic coordinates for each of the $n_x \times n_y$ pixels. Each element of the array consists of a latitude-longitude pair $\left(\lambda_g, \varphi_g \right)$.

M, an n_x by n_y dimensional array containing the geomagnetic coordinates for each of the $n_x \times n_y$ pixels. Each element of the array consists of a latitude-longitude pair $\left(\lambda_m, \varphi_m \right)$.

ψ, an n_x by n_y dimensional array containing the nadir angle ψ for each of the $n_x \times n_y$ pixels.

OUTPUT:

$\mathbf{S} = \left[S_1, S_2, ... S_{N_s} \right]$, the vector of pixel indices corresponding to each of the N_s spectra. Each element, S_i, of the vector consists of a pair of integers (m, n) giving the column number and row number of the pixel contain the foot of the corresponding field line.

N_{ss}, the number of distinct subsatellite pixels. Generally, N_{ss} is less than N_s.

$\mathbf{P} = \left[P_1, P_2, ... P_{N_{ss}} \right]$, a vector containing the N_{ss} distinct pixel indices. P is just S with duplicates removed.

Procedure:

Step 1: Locate boundaries

Definition: $\mathbf{B}_h = \left[B_{eq1}, B_{pl1}, B_{eq2}, B_{pl2} \right]$ are the indices of the spectra that mark the boundaries of the auroral precipitation

Definition:

Details of procedure TBD.

Step 2: Trace field lines

$N_{ss} = 0$

For $i = 1$ to N_s do

Begin Field Line Trace at the position $(\lambda_i, \varphi_i, h_i)$

[Precise field line tracing algorithm depends on the magnetic field model chosen.]

End Field Line Trace when $z = 110$ km

Begin Pixel Search

[Precise pixel search algorithm is TBD.]

End Pixel Search when pixel containing foot of field line is found

$S_i = (m, n)$

If $i \neq 1$ then

    If $S_i \neq S_j, \quad j = 1, 2, \ldots i - 1$ then

        $N_{ss} = N_{ss} + 1$

        $P_{N_{ss}} = S_i$

    End If

    Else

        $N_{ss} = 1$

        $P_1 = S_1$

    End If

End For

End Procedure

END MODULE 2.

4.3 Sensor fusion analysis of subsatellite pixel data

Since the characteristics of the precipitating particles (electrons and protons) are known for these pixels, the intensities of the four spectral regions (121.6 nm, 125.6 nm, LBH1, and LBH2) sampled by the SSUSI instrument can be predicted. However, the predictions depend on assumptions about the neutral composition, in particular the relative column abundances of N_2, O, and O_2. Therefore, any differences between the predicted intensities and the observed intensities may be interpreted in terms of departures of the actual atmospheric composition from the assumed composition.

MODULE 3: Sensor fusion data analysis

PURPOSE: To deduce O/N2 and O2/N2 ratios by comparing the observed intensities with the intensities expected from the measured electron and ion spectra.

INPUT:

    N_s, **the number of electron and/or ion spectra taken during the same time interval as the image**

    $\tau = \left[\tau_1, \tau_2, \ldots \tau_{N_s}\right]$, **the vector of times (UT) corresponding to each of the N_s spectra**

$\lambda = \left[\lambda_1, \lambda_2, \ldots \lambda_{N_s}\right]$, the vector of satellite geographic latitudes corresponding to each of the N_s spectra

$\varphi = \left[\varphi_1, \varphi_2, \ldots \varphi_{N_s}\right]$, the vector of satellite geographic longitudes corresponding to each of the N_s spectra

$\mathbf{C}^{(e)} = \left[\mathbf{C}_1^{(e)}, \mathbf{C}_2^{(e)}, \ldots \mathbf{C}_{N_s}^{(e)}\right]$, the vector of electron spectra characteristics as determined by the SSJ/5 data analysis module. Each element of the vector is an eight element vector:

$$\mathbf{C}_j^{(e)} = \left[ST_{e,j}, E_{0e,j}, Q_{0e,j}, E_{MS,j}, SP_{e,j}, E_{1e,j}, Q_{1e,j}, W_{1e,j}\right]$$

$\mathbf{C}^{(p)} = \left[\mathbf{C}_1^{(p)}, \mathbf{C}_2^{(p)}, \ldots \mathbf{C}_{N_s}^{(p)}\right]$, the vector of proton spectra characteristics as determined by the SSJ/5 data analysis module. Each element of the vector is a two element vector: $\mathbf{C}_j^{(p)} = \left[E_{0p,j}, Q_{0p,j}\right]$.

G, an n_x by n_y dimensional array containing the geographic coordinates for each of the $n_x \times n_y$ pixels. Each element of the array consists of a latitude-longitude pair $\left(\lambda_g, \varphi_g\right)$.

M, an n_x by n_y dimensional array containing the geomagnetic coordinates for each of the $n_x \times n_y$ pixels. Each element of the array consists of a latitude-longitude pair $\left(\lambda_m, \varphi_m\right)$.

ψ, an n_x by n_y dimensional array containing the nadir angle ψ for each of the $n_x \times n_y$ pixels.

$\mathbf{I}_{1216}$, an n_x by n_y dimensional array containing the 121.6 nm intensity I_{1216} for each of the $n_x \times n_y$ pixels

$\mathbf{I}_{1356}$, an n_x by n_y dimensional array containing the 135.6 nm intensity I_{1356} for each of the $n_x \times n_y$ pixels

$\mathbf{I}_{LBH1}$, an n_x by n_y dimensional array containing the LBH1 intensity I_{LBH1} for each of the $n_x \times n_y$ pixels

$\mathbf{I}_{LBH2}$, an n_x by n_y dimensional array containing the LBH2 intensity I_{LBH2} for each of the $n_x \times n_y$ pixels

N_{ss}, the number of distinct subsatellite pixels. Generally, N_{ss} is less than N_s.

$\mathbf{P} = \left[P_1, P_2, \ldots P_{N_{ss}}\right]$, a vector containing the N_{ss} distinct pixel indices. P is just S with duplicates removed.

$\mathbf{S} = \left[S_1, S_2, \ldots S_{N_s}\right]$, the vector of pixel indices corresponding to each of the N_s spectra. Each element, S_i, of the vector consists of a pair of integers (m, n) giving the column number and row number of the pixel contain the foot of the corresponding field line.

OUTPUT:

N_x, the number of intervals in the normalized latitudinal coordinate x defined below.

$\mathbf{x} = \left[x_0, x_1, \dots x_{N_x} \right]$, the vector of x coordinate values, where x is a normalized latitudinal coordinate such that at the equatorward auroral boundary $x = x_0 = 0$ and at the poleward auroral boundary $x = x_{N_x} = 1$

$\boldsymbol{\eta}^{(O)} = \left[\eta_1^{(O)}, \eta_2^{(O)}, \dots \eta_{N_x}^{(O)} \right]$, the vector of atomic oxygen (O) scale factors necessary to bring the predicted intensities in line with the observed intensities. Each element of the vector consists of a two element vector corresponding to the two local times at which the satellite cuts the auroral oval: $\eta_j^{(O)} = \left[\eta_j^{(O)}(T_1), \eta_j^{(O)}(T_2) \right]$.

$\boldsymbol{\eta}^{(O_2)} = \left[\eta_1^{(O_2)}, \eta_2^{(O_2)}, \dots \eta_{N_x}^{(O_2)} \right]$, the vector of atomic oxygen (O_2) scale factors necessary to bring the predicted intensities in line with the observed intensities. Each element of the vector consists of a two element vector corresponding to the two local times at which the satellite cuts the auroral oval: $\eta_j^{(O_2)} = \left[\eta_j^{(O_2)}(T_1), \eta_j^{(O_2)}(T_2) \right]$.

$\mathbf{T} = \left[T_1, T_2 \right]$, a two element vector containing the two nominal local times at which these scale factors apply.

Procedure:

Definition: N_p is the number of electron and ion spectra corresponding to a single subsatellite pixel.

Definition: $\Sigma \mathbf{C}^{(e)}$ is an eight element vector containing the sum of the electron characteristics for the N_p spectra corresponding to a single subsatellite pixel.

Definition: $\Sigma \mathbf{C}^{(p)}$ is a two element vector containing the sum of the proton characteristics for the N_p spectra corresponding to a single subsatellite pixel.

Definition: $\mathbf{C}_p^{(e)}$ is an eight element vector containing the average electron characteristics for a single subsatellite pixel.

Definition: $\mathbf{C}_p^{(p)}$ is a two element vector containing the average proton characteristics for a single subsatellite pixel.

Definition: $\mathbf{I} = \left[I_{1216}(m,n), I_{1356}(m,n), I_{LBH1}(m,n), I_{LBH2}(m,n) \right]$ is a four element vector containing the observed intensities for a single pixel.

Definition: $\mathbf{R} = \left[R_O, R_{O_2} \right]$ is a two element vector containing scale factors for O and O_2.

Definition: **RADJ** is a function procedure that determines the best values for $\mathbf{R}$.

Definition: $\mathbf{x_s} = \left[x_{s,1}, x_{s,2}, \dots x_{s,N_s} \right]$ is a vector containing the normalized x coordinates for each of the N_s spectra.

Definition: $\boldsymbol{\eta}_s^{(O)} = \left[\eta_{s,1}^{(O)}, \eta_{s,2}^{(O)}, \dots \eta_{s,N_s}^{(O)} \right]$ is a vector containing the O scale factors at $\mathbf{x}_s$.

Definition: $\boldsymbol{\eta}_s^{(O_2)} = \left[\eta_{s,1}^{(O_2)}, \eta_{s,2}^{(O_2)}, \dots \eta_{s,N_s}^{(O_2)} \right]$ is a vector containing the O_2 scale factors at $\mathbf{x}_s$.

For $i = 1, N_{ss}$ do

$N_p = 0$

$\Sigma \mathbf{C}^{(e)} = 0$

$\Sigma \mathbf{C}^{(p)} = 0$

Determine how many electron and ion spectra correspond to this pixel.

For $j = 1, N_s$ do

    If $S_j = P_i$ then

        $k = k + 1$

        $\Sigma \mathbf{C}^{(e)} = \Sigma \mathbf{C}^{(e)} + \mathbf{C}_j^{(e)}$

        $\Sigma \mathbf{C}^{(p)} = \Sigma \mathbf{C}^{(p)} + \mathbf{C}_j^{(p)}$

    End If

End For

$\mathbf{C}_p^{(e)} = \dfrac{\Sigma \mathbf{C}^{(e)}}{N_p}$

$\mathbf{C}_p^{(p)} = \dfrac{\Sigma \mathbf{C}^{(p)}}{N_p}$

$\mathbf{I} = \left[I_{1216}(P_i), I_{1356}(P_i), I_{LBH1}(P_i), I_{LBH2}(P_i) \right]$

$\mathbf{R} = \mathbf{RADJ}\left(\mathbf{C}_p^{(e)}, \mathbf{C}_p^{(p)}, \mathbf{I} \right)$ {NOTE: **RADJ** will probably require additional arguments}

$x_i = \dfrac{\lambda_i - \lambda_{eq}}{\lambda_{pl} - \lambda_{eq}}$

$\eta_{s,i}^{(O)} = R_O$

$\eta_{s,i}^{(O_2)} = R_{O_2}$

End For

$\eta^{(O)} = \mathbf{INTRP}\left(\mathbf{x}_s, \eta_s^{(O)}, \mathbf{x} \right)$

$\eta^{(O_2)} = \mathbf{INTRP}\left(\mathbf{x}_s, \eta_s^{(O_2)}, \mathbf{x} \right)$

End Procedure

END MODULE 3.

5. SSUSI Off-Track Data Analysis Module

This module processes the off-track pixel data ingest by the Subsatellite module.

5.1 Data analysis of off-track pixel data

Since the characteristics of the precipitating particles (electrons and protons) are known for these pixels, the intensities of the four spectral regions (121.6 nm, 125.6 nm, LBH1, and LBH2) sampled by the SSUSI instrument can be predicted. However, the predictions depend on assumptions about the neutral composition, in particular the relative column abundances of N_2, O, and O_2. Therefore, any differences between the predicted intensities and the observed intensities may be interpreted in terms of departures of the actual atmospheric composition from the assumed composition.

MODULE 1: Off-track pixel data analysis

PURPOSE: To deduce electron and proton characteristics from the SSUSI image data.

INPUT:
    G, an n_x by n_y dimensional array containing the geographic coordinates for each of the
        $n_x \times n_y$ pixels. Each element of the array consists of a latitude-longitude pair (λ_g, φ_g).
    M, an n_x by n_y dimensional array containing the geomagnetic coordinates for each of the
        $n_x \times n_y$ pixels. Each element of the array consists of a latitude-longitude pair (λ_m, φ_m).
    T, an n_x by n_y dimensional array containing the local time for each of the $n_x \times n_y$ pixels.
    $\mathbf{I}_{1216}$, an n_x by n_y dimensional array containing the 121.6 nm intensity I_{1216} for each of the
        $n_x \times n_y$ pixels
    $\mathbf{I}_{1356}$, an n_x by n_y dimensional array containing the 135.6 nm intensity I_{1356} for each of the
        $n_x \times n_y$ pixels
    $\mathbf{I}_{LBH1}$, an n_x by n_y dimensional array containing the LBH1 intensity I_{LBH1} for each of the
        $n_x \times n_y$ pixels
    $\mathbf{I}_{LBH2}$, an n_x by n_y dimensional array containing the LBH2 intensity I_{LBH2} for each of the
        $n_x \times n_y$ pixels
    N_{ss}, the number of distinct subsatellite pixels.
    $\mathbf{P}^{(ss)} = \left[P_1^{(ss)}, P_2^{(ss)}, \ldots P_{N_{ss}}^{(ss)} \right]$, a vector containing the N_{ss} distinct pixel indices.
    N_x, the number of intervals in the normalized latitudinal coordinate x defined below.
    $\mathbf{x} = \left[x_0, x_1, \ldots x_{N_x} \right]$, the vector of x coordinate values, where x is a normalized latitudinal
                coordinate such that at the equatorward auroral boundary $x = x_0 = 0$ and at
                the poleward auroral boundary $x = x_{N_x} = 1$

$\eta^{(O)} = \left[\eta_1^{(O)}, \eta_2^{(O)}, \dots \eta_{N_x}^{(O)} \right]$, the vector of atomic oxygen (O) scale factors necessary to bring the predicted intensities in line with the observed intensities. Each element of the vector consists of a two element vector corresponding to the two local times at which the satellite cuts the auroral oval: $\eta_j^{(O)} = \left[\eta_j^{(O)}(T_1), \eta_j^{(O)}(T_2) \right]$.

$\eta^{(O_2)} = \left[\eta_1^{(O_2)}, \eta_2^{(O_2)}, \dots \eta_{N_x}^{(O_2)} \right]$, the vector of atomic oxygen (O$_2$) scale factors necessary to bring the predicted intensities in line with the observed intensities. Each element of the vector consists of a two element vector corresponding to the two local times at which the satellite cuts the auroral oval: $\eta_j^{(O_2)} = \left[\eta_j^{(O_2)}(T_1), \eta_j^{(O_2)}(T_2) \right]$.

$\mathbf{T}^{(\eta)} = \left[T_1^{(\eta)}, T_2^{(\eta)} \right]$, a two element vector containing the two nominal local times at which these scale factors apply.

OUTPUT:

$\mathbf{ST}_e$, an n_x by n_y dimensional array containing the electron energy spectra type for each of the $n_x \times n_y$ pixels

$\mathbf{E}_{0e}$, an n_x by n_y dimensional array containing the characteristic electron energy for each of the $n_x \times n_y$ pixels

$\mathbf{Q}_{0e}$, an n_x by n_y dimensional array containing the downward electron energy flux each of the $n_x \times n_y$ pixels

$\mathbf{E}_{SM}$, an n_x by n_y dimensional array containing the Maxwellian characteristic energy for shifted Maxwellians for each of the $n_x \times n_y$ pixels

$\mathbf{E}_{0p}$, an n_x by n_y dimensional array containing the characteristic proton energy for each of the $n_x \times n_y$ pixels

$\mathbf{Q}_{0p}$, an n_x by n_y dimensional array containing the downward proton energy flux each of the $n_x \times n_y$ pixels

Procedure:

Step 1: Determine auroral boundaries
   Apply SSUSI Single Sensor boundary algorithm.
   Apply boundary tracing algorithm to produce ordered list of boundary pixels.
   If boundaries intersect image border, fit smooth curve to estimate boundary location outside of pixel.
   Produce vector $\mathbf{b}_{eq}$ and $\mathbf{b}_{pl}$ to tabulate equatorward and poleward boundary as a function of local time, $\mathbf{T}_b$.

Step 2: Process pixels.

For $i = 1$ to n_x do

    For $j = 1$ to n_y do

        $P_{ij} = (i, j)$

        $SS_{ij} = $ FALSE

        $k = 0$

        Repeat

            $k = k + 1$

            If $P_{ij} = P_k^{(ss)}$ Then $SS_{ij} = $ TRUE

        Until $SS_{ij} = $ TRUE or $k = N_{ss}$

        If $SS_{ij} = $ TRUE Then

            This is a subsatellite pixel, use the measured electron and proton characteristics.

        Else

            This is not a subsatellite pixel, calculate the electron and proton characteristics.

            Ascertain equatorward and poleward boundaries for this local time:

            $\lambda_{eq} = \text{INTRP}(\mathbf{b}_{eq}, \mathbf{T}_b, T_{ij})$

            $\lambda_{pl} = \text{INTRP}(\mathbf{b}_{pl}, \mathbf{T}_b, T_{ij})$

            $x_{ij} = \dfrac{\lambda_{ij} - \lambda_{eq}}{\lambda_{pl} - \lambda_{eq}}$

            $R_O = \text{INTRP}(\eta^{(O)}, \mathbf{x}, x_{ij})$

            $R_{O_2} = \text{INTRP}(\eta^{(O_2)}, \mathbf{x}, x_{ij})$

            First Stage Analysis (assume Maxwellian electron spectra):

                $\text{NONLIN}(\text{"Maxwell"}, R_O, R_{O_2}, I_{1216}, I_{1356}, I_{LBH1}, I_{LBH2}; E_{0e}, Q_{0e}, E_{0p}, Q_{0p})$

            End First Stage Analysis

            Second Stage Analysis:

                If $Q_{0p} < 0.05 Q_{0e}$ Then

                    Pure electron aurora

                Else If $Q_{0p} \leq 20 Q_{0e}$ Then

                    Combined electron and proton aurora

                    If $Q_{0e} \leq Q_{threshold}$ Then

                        Stage 1 Analysis OK: Do nothing

                    Else

                      Redo Stage 1 Analysis using monoenergetic electrons

                      $\text{NONLIN}(\text{"Mono"}, R_O, R_{O_2}, I_{1216}, I_{1356}, I_{LBH1}, I_{LBH2}; E_{0e}, Q_{0e}, E_{0p}, Q_{0p})$

                  End If

                Else

                  Pure proton aurora

                End If

            End Second Stage Analysis

        End If

End For
End For

End Procedure

END MODULE 1.

5.2 Refinements

In future version of the algorithm, it may be possible to refine the analysis by interpolating the $\eta^{(O)}$ and $\eta^{(O_2)}$ functions using values generated by the pure electron and pure proton analysis.

6. Auroral E-layer electron density profile parameters

This module uses the electron and proton characteristics and the neutral composition data determined by the previous modules to estimate $N_m E$ and $h_m E$.

Ionization is produced by electron impact, proton impact, and photon impact. The processes are linear so the total production rate of ions is just the sum of the production rates from the three processes. The electron density is obtained using a simple chemical model with an effective recombination rate. Unlike the single sensor algorithm, which used a single altitude profile for the recombination rate, the new algorithm allows the recombination rate to depend on neutral composition.

MODULE 1: Calculation of Auroral E-layer parameters.

PURPOSE: To calculate the E-layer parameters $N_m E$ and $h_m E$.

INPUT:

n_x, the number of columns of pixels in the image.

n_y, the number of rows of pixels in the image.

Q_{EUV}, the incident solar EUV flux (erg cm^{-2} s^{-1}) as determined by the SSUSI single sensor algorithm.

$\mathbf{G}$, an n_x by n_y dimensional array containing the geographic coordinates for each of the $n_x \times n_y$ pixels. Each element of the array consists of a latitude-longitude pair $\left(\lambda_g, \varphi_g\right)$.

$\mathbf{M}$, an n_x by n_y dimensional array containing the geomagnetic coordinates for each of the $n_x \times n_y$ pixels. Each element of the array consists of a latitude-longitude pair $\left(\lambda_m, \varphi_m\right)$.

$\mathbf{T}$, an n_x by n_y dimensional array containing the local time for each of the $n_x \times n_y$ pixels.

χ, an n_x by n_y dimensional array containing the solar zenith angle for each of the $n_x \times n_y$ pixels.

$\eta^{(O)}$, an n_x by n_y dimensional array containing the atomic oxygen (O) scale factors for each of the $n_x \times n_y$ pixels.

$\eta^{(O_2)}$, an n_x by n_y dimensional array containing the molecular oxygen (O$_2$) scale factors for each of the $n_x \times n_y$ pixels.

ST$_e$, an n_x by n_y dimensional array containing the electron energy spectra type for each of the $n_x \times n_y$ pixels

E$_{0e}$, an n_x by n_y dimensional array containing the characteristic electron energy for each of the $n_x \times n_y$ pixels

Q$_{0e}$, an n_x by n_y dimensional array containing the downward electron energy flux each of the $n_x \times n_y$ pixels

E$_{SM}$, an n_x by n_y dimensional array containing the Maxwellian characteristic energy for shifted Maxwellians for each of the $n_x \times n_y$ pixels

E$_{0p}$, an n_x by n_y dimensional array containing the characteristic proton energy for each of the $n_x \times n_y$ pixels

Q$_{0p}$, an n_x by n_y dimensional array containing the downward proton energy flux for each of the $n_x \times n_y$ pixels

OUTPUT:

N$_m$E, an n_x by n_y dimensional array containing peak E-layer electron density (cm^{-3}) for each of the $n_x \times n_y$ pixels

h$_m$E, an n_x by n_y dimensional array containing the height of the E-layer (km) for each of the $n_x \times n_y$ pixels

Procedure:

Definition: h_e is the height (km) of the peak ionization due to electron impact.

Definition: h_p is the height (km) of the peak ionization due to proton impact.

Definition: $h_{ph} = 108$ km is the height of the peak photoionization rate at the subsolar point.

Definition: P_e is the peak ionization rate (cm^{-3} s^{-1}) due to electron impact.

Definition: P_p is the peak ionization rate (cm^{-3} s^{-1}) due to proton impact.

Definition: H_e is a scale height (km) that defines the shape of the Chapman function that describes the altitude dependence of the electron impact ionization rate.

Definition: H_p is a scale height (km) that defines the shape of the Chapman function that describes the altitude dependence of the proton impact ionization rate.

Definition: $H_{ph} = 9$ km is the neutral scale height near h_{ph}. It defines the shape of the Chapman function that describes the altitude dependence of the photoionization rate.

Definition: N_z is the number of points on the predefined altitude grid used in the algorithm.

Definition: $\mathbf{z} = [z_1, z_2, \ldots z_{N_z}]$ is the predefined altitude grid on which the electron density profile is calculated prior to locating the peak density.

Definition: u_e is the reduced height used in the calculation of the electron impact ionization altitude profile.

Definition: u_p is the reduced height used in the calculation of the proton impact ionization altitude profile.

Definition: u_{ph} is the reduced height used in the calculation of the photoionization altitude profile.

Definition: p_e is the electron impact ionization rate at a specified altitude.

Definition: p_p is the proton impact ionization rate at a specified altitude.

Definition: p_{ph} is the photoionization rate at a specified altitude.

Definition: $\mathbf{n} = [n_1, n_2, \ldots n_{N_z}]$ is a vector containing the electron densities corresponding to the altitudes $\mathbf{z}$.

Definition: α is the effective recombination rate at a specified altitude.

Definition: HEIGHT is a function procedure that calculates the height of the ionization peak from the particle characteristics. The argument list depends on the type of particle.

Definition: PEAK is a function procedure that calculates the peak ionization rate for an energy flux of 1 erg cm^{-2} s^{-1} given the particle characteristics. The argument list depends on the type of particle.

Definition: Ch is a function procedure that calculates the Chapman Grazing Incidence function. The argument is the solar zenith angle. $\mathrm{Ch}(0) = 1$.

Definition: CHAPMAN is a function procedure that calculates a Chapman function, S, of the form

$$S(u, \chi) = \exp\left[1 - u - e^{-u}\mathrm{Ch}(\chi)\right]$$

Definition: RECOMB is a function procedure that calculates the effective recombination rate as a function of altitude and neutral composition.

For $i = 1$ to n_x do

    For $j = 1$ to n_y do

        $h_e = \mathrm{HEIGHT}("\text{electron}", ST_e, E_{0e})$

        $h_p = \mathrm{HEIGHT}("\text{proton}", E_{0p})$

        $P_e = Q_{0e} \times \mathrm{PEAK}("\text{electron}", ST_e, E_{0e}, E_{SM})$

        $P_e = Q_{0p} \times \mathrm{PEAK}("\text{proton}", E_{0p})$

        $H_e = \dfrac{5.25 \times 10^{10}}{P_e}$

        $H_p = \dfrac{8.46 \times 10^{10}}{P_p}$

        For $k = 1$ to N_z do

$$u_e = \frac{z_k - h_e}{H_e}$$

$$u_p = \frac{z_k - h_p}{H_p}$$

$$u_{ph} = \frac{z_k - h_{ph}}{H_{ph}}$$

$$p_e = P_e \times \text{CHAPMAN}(u_e, 0)$$

$$p_p = P_p \times \text{CHAPMAN}(u_p, 0)$$

$$p_{ph} = Q_{EUV} \times \text{CHAPMAN}(u_{ph}, \chi)$$

$$\alpha = \text{RECOMB}\left(z_k, \eta_{ij}^{(O)}, \eta_{ij}^{(O_2)}\right)$$

$$n_k = \sqrt{\frac{p_e + p_p + p_{ph}}{\alpha}}$$

End For

$$N_m E_{ij} = \text{MAX}(\mathbf{n}, k_{max})$$

$$h_m E_{ij} = z_{k_{max}}$$

End For

End For

End Procedure

END MODULE 1.

REFERENCES

Daniell, R. E., and D. J. Strickland, Dependence of auroral middle UV emissions on the incident electron spectrum and neutral atmosphere, *J. Geophys. Res.*, *91*, 321-327, 1986.

Daniell, R. E., D. J. Strickland, D. T. Decker, J. R. Jasperse, and H. C. Carlson, Determination of Ionospheric Electron Density Profiles From Satellite UV Emission Measurements, FY84, AFGL-TR-85-0099, 1985, ADA160368.

Daniell, R. E., W. G. Whartenby, and L. D. Brown, SSUSI Single Sensor Auroral E-layer Algorithm: Functional Description, PL-TR-94-2195, 1994, ADA288630.

Hoffman, R. A., From balloons to chemical releases—What do charge particles tell us about the auroral potential region? in *Auroral Plasma Dynamics*, Robert L. Lysak, editor, American Geophysical Union, Washington, pp. 133-142, 1993.

Strickland, D. J., J. R. Jasperse, and J. A. Whalen, Dependence of auroral FUV emissions on the incident electron spectrum and neutral atmosphere, *J. Geophys. Res.*, *88*, 8051-8062, 1983.

Strickland, D. J., R. E. Daniell, D. T. Decker, J. R. Jasperse, and H. C. Carlson, Determination of Ionospheric Electron Density Profiles from Satellite UV Emission Measurements, AFGL-TR-84-0140, 1984, ADA150734.

Strickland, D. J., R. E. Daniell, J. R. Jasperse, and B. Basu, Transport-theoretic model for the electron-proton-hydrogen atom aurora, 2. Model results, *J. Geophys. Res.*, *98*, 21,533-21,548, 1993.